Systems & Control Letters 193 (2024) 105907

Contents lists available at ScienceDirect

Systems & Control Letters

journal homepage: www.elsevier.com/locate/sysconle

Competitive epidemic networks with multiple survival-of-the-fittest outcomes☆

Mengbin Ye [a,*], Brian D.O. Anderson [b], Axel Janson [c], Sebin Gracy [d], Karl H. Johansson [e]

[a] Centre for Optimisation and Decision Science, Curtin University, Perth, Australia
[b] School of Engineering, Australian National University, Canberra, Australia
[c] Department of Mathematics, School of Engineering Sciences, KTH Royal Institute of Technology, Stockholm, Sweden
[d] Department of Electrical Engineering and Computer Science, South Dakota School of Mines and Technology, SD, USA
[e] Division of Decision and Control Systems, School of Electrical Engineering and Computer Science, KTH Royal Institute of Technology, and Digital Futures, Stockholm, Sweden

ARTICLE INFO

Keywords:
Susceptible–infected–susceptible (SIS)
Bivirus
Stability of nonlinear systems
Monotone systems

ABSTRACT

We use a deterministic model to study two competing viruses spreading over a two-layer network in the Susceptible–Infected–Susceptible (SIS) framework, and address a central problem of identifying the winning virus in a "survival-of-the-fittest" battle. Almost all existing conditions ensure that the same virus wins regardless of initial states. In the present paper, we ask the following question: can we systematically construct SIS bivirus networks with an arbitrary but finite number of nodes such that *either* of the viruses can win the survival-of-the-fittest battle, depending on the initial states? We answer this question in the affirmative. More specifically, we show that given almost any network layer of one virus, we can (using our proposed systematic four-step procedure) construct the network layer for the other virus such that in the resulting bivirus network, either of the two viruses can win the survival-of-the-fittest battle. Conclusions from numerical case studies, including a real-world mobility network that captures the commuting patterns for people between 107 provinces in Italy, illustrate and extend the theoretical result and its consequences.

1. Introduction

Mathematical models of epidemics have been studied extensively for over two centuries, providing insight into the process by which infectious diseases and viruses spread across human or other biological populations [1,2]. Models utilizing health compartments are classical, where each individual in a large population may be susceptible to the virus (S), infected with the virus and able to infect others (I), or removed with permanent immunity through recovery or death (R). Different diseases or viruses are modeled by including different compartments and specifying the possible transitions between the compartments. Two classical frameworks are Susceptible–Infected–Removed (SIR) and Susceptible–Infected–Susceptible (SIS), while further compartments can be added to reflect latent or incubation periods for the disease, or otherwise provide a more realistic description of the epidemic process. Moving beyond single populations, network models of meta-populations have also been widely studied, where each node in the network represents a large population and links represent the potential for the virus to spread between nodes.

Recently, increasing attention has been directed to network models of epidemics involving two or more viruses [3,4]. Depending on the problem scenario, the viruses may be cooperative; being infected with one virus makes an individual more vulnerable to infection from another virus [5–7]. Alternatively, viruses may be competitive, whereby being infected with one virus can provide an individual with partial or complete protection from also being infected with another virus. The focus of the present paper is on the competitive networked bivirus SIS model. This model is a deterministic continuous-time dynamical system [8–12]. The two viruses, termed virus 1 and virus 2, spread across a two-layer meta-population network; each layer represents the possibly distinct topologies for virus 1 and virus 2. In each population, individuals belong to one of three mutually exclusive compartments: infected by virus 1, or infected by virus 2, or not infected by either of the viruses. The competing nature implies that an individual infected

☆ M. Ye is supported by the Western Australian Government through the Premier's Science Fellowship Program, and by the Australian Government through the Office of National Intelligence (NI240100203). The work of A.J., S.G, and K.H.J. is supported in part by a Knut and Alice Wallenberg Foundation Wallenberg Scholar Grant, a Swedish Research Council Distinguished Professor Grant, and the Swedish Strategic Research Foundation SUCCESS Grant (FUS21-0026).

* Corresponding author.
E-mail address: mengbin.ye@curtin.edu.au (M. Ye).

https://doi.org/10.1016/j.sysconle.2024.105907
Received 18 January 2023; Received in revised form 30 May 2024; Accepted 14 August 2024
Available online 2 September 2024

by virus 1 cannot be infected by virus 2, and vice versa. An infected individual that recovers from either virus will do so with no immunity, and then becomes susceptible again to infection from either virus. In this context, a central question is whether each virus will persist over time or become extinct [8–11,13–22]. If a particular virus persists while others become extinct, it is said to have won the "survival-of-the-fittest" battle [8,23]. Assuming both the viruses are present initially, an important problem is as follows: Which of the two viruses will win the survival-of-the-fittest battle?

Existing literature on bivirus networks has identified a variety of scenarios that specify the winning virus in a survival-of-the-fittest battle [9–12,18–20]. Importantly, most results are solely parameter-dependent [9–12,18–20]; these papers establish sufficient conditions on the parameters so that the identity of the winning virus is *independent* of the initial states (initial infection level). See, for instance, [20, Theorem 6], [12, Corollary 3.11, statements 1 and 2]. In this paper, we consider a different key yet relatively unexplored scenario: *networks for which either virus can prevail in the survival-of-the-fittest battle, depending on the initial states.* Ref. [8] provided a comprehensive analysis of a 3-node graph with a specialized structure, including identifying a necessary and sufficient condition for either of the viruses to prevail, depending on the initial states [8, Theorem 3.2]. The condition in [8, Theorem 3.2] was recently extended for bivirus networks with (a) arbitrary but finite number of n nodes, and (b) arbitrary (but strongly connected) graph structures [12, Theorem 3.10]. The satisfaction or otherwise of said condition can result in multiple possibilities with respect to the dynamical behavior of the bivirus system; see Scenarios 1–3 in Section 2.

A key reason for the lack of developed theory regarding networks with different possible winning viruses is that numerical examples (which can be used to guide theoretical analysis) are lacking. This is because the conditions, such as in [12, Theorem 3.10], are expressed implicitly as complex nonlinear functions of the model parameters. In other words, although it is straightforward to check whether a given bivirus network satisfies the conditions in [12, Theorem 3.10], the converse problems of establishing *existence* and of *designing* such networks are significantly more challenging. Indeed, apart from the specialized $n = 3$ network studied in [8], it was only recently that $n = 2$ and $n = 4$ example networks were identified [12,24]. There is also no insight as to whether for networks with an arbitrary number of nodes, apart from the cases already covered, there even exist bivirus networks where the winning virus in a survival-of-the-fittest battle depends on the initial states. A theoretical argument and accompanying procedure for generating networks would significantly enhance our technical understanding of bivirus spread, given that scenarios in which both viruses can prevail underpin some of the central questions in mathematical epidemiology. The present paper aims to address these issues.

We prove that, given almost any network layer of virus 1 (resp. virus 2), there always exists a network layer of virus 2 (resp. virus 1) such that the resulting bivirus network satisfies the necessary and sufficient conditions in [12, Theorem 3.10]; see Theorem 1. This provides a conclusive answer to the existence problem, i.e. for an arbitrary number of n nodes, there always exist networks where the winning virus depends on the initial states. We subsequently operationalize the theoretical results by developing a robust four-step procedure, starting with an essentially arbitrary network layer corresponding to the spread of virus 1 (resp. virus 2), to construct the other network layer corresponding to the spread of virus 2 (resp. virus 1) so as to satisfy the aforementioned condition. This addresses a second issue highlighted above, by allowing one to generate and then study bivirus networks that have two possible survival-of-the-fittest outcomes. Taken as a whole, our work offers deeper insight into bivirus networks and the complex survival-of-the-fittest battles that unfold over them.

Paper outline

We conclude this section by collecting most of the notations and certain preliminaries required in the sequel. The bivirus network model is detailed in Section 2, where we also formulate the problem of interest. The main results are presented in Section 3; the proofs have been relegated to the Appendix. Two case studies that illustrate the construction procedure and the resulting diverse limiting behavior are provided in Section 4. Finally, conclusions and potential future work are given in Section 5.

Notation and preliminaries

We use I to denote the identity matrix, with dimension to be understood from the context. Let A be a square matrix, with eigenvalues λ_i. We use $\rho(A) = \max_i |\lambda_i|$ and $\sigma(A) = \max_i \Re\mathfrak{e}(\lambda_i)$ to denote the spectral radius and the spectral abscissa of A, respectively. If $\sigma(A) < 0$, we say A is Hurwitz. The matrix A is reducible if and only if there is a permutation matrix P such that $P^\top AP$ is block upper triangular; otherwise A is said to be irreducible. For two vectors $x = \{x_i\}$ and $y = \{y_i\}$ of the same dimension, we write $x \le y \Leftrightarrow x_i \le y_i$ for all i, and $x < y \Leftrightarrow x_i < y_i$ for all i. We use $\mathbf{0}_n$ and $\mathbf{1}_n$ to denote the all-0 and all-1 column vectors of dimension n. We define the set

$$\Delta = \{(x, y) \in \mathbb{R}^n_{\ge 0} \times \mathbb{R}^n_{\ge 0} : \mathbf{0}_n \le x + y \le \mathbf{1}_n\},$$

and its interior by $\mathrm{Int}(\Delta)$.

In this paper, we consider two-layer directed networks represented by the graph $\mathcal{G} = (\mathcal{V}, \mathcal{E}_A, \mathcal{E}_B)$, where $\mathcal{V} = \{1, \dots, n\}$ is the set of nodes, and $\mathcal{E}_A \subseteq \mathcal{V} \times \mathcal{V}$ and $\mathcal{E}_B \subseteq \mathcal{V} \times \mathcal{V}$ are the ordered set of edges of the first and second layer, respectively. Associated with $\mathcal{E}_A$ and $\mathcal{E}_B$ are the nonnegative adjacency matrices $A = \{a_{ij}\}$ and $B = \{b_{ij}\}$, respectively. We define $a_{ij} > 0$ and $b_{ij} > 0$ if and only if $(j, i) \in \mathcal{E}_A$ and $(j, i) \in \mathcal{E}_B$, respectively, where (j, i) is the directed edge from node j to node i. A layer is strongly connected if and only if there is a path from any node i to any other node j, which corresponds to the associated adjacency matrix being irreducible [25].

2. Bivirus network model

Following the convention in the literature [9], we consider two viruses spreading over a two-layer network represented by the graph $\mathcal{G} = (\mathcal{V}, \mathcal{E}_A, \mathcal{E}_B)$, where $\mathcal{E}_A$ and $\mathcal{E}_B$ determine the spreading topology for virus 1 and virus 2, respectively. Each node represents a well-mixed population of individuals with a large and constant size; a well-mixed population means any two individuals in the population can interact with the same positive probability. Fig. 1 shows a schematic of the compartment transitions, and the two-layer network structure.

We define $x_i(t) \in [0, 1]$ and $y_i(t) \in [0, 1]$, $t \in \mathbb{R}_+$, as the fraction of individuals in population $i \in \mathcal{V}$ infected with virus 1 and virus 2, respectively. In accordance with [9–11], the dynamics at node $i \in \mathcal{V}$ are given by

$$\dot{x}_i(t) = -x_i(t) + (1 - x_i(t) - y_i(t)) \textstyle\sum_{j=1}^n a_{ij} x_j(t) \tag{1a}$$

$$\dot{y}_i(t) = -y_i(t) + (1 - x_i(t) - y_i(t)) \textstyle\sum_{j=1}^n b_{ij} y_j(t), \tag{1b}$$

with $a_{ij} \ge 0$ and $b_{ij} \ge 0$ being infection rate parameters. In fact, individuals in population j infected with virus 1 (resp. virus 2) can infect susceptible individuals in population i if and only if $(j, i) \in \mathcal{E}_A$ (resp. $\mathcal{E}_B$) at a rate a_{ij} (resp. b_{ij}). By defining $x(t) = [x_1(t), \dots, x_n(t)]^\top$ and $y(t) = [y_1(t), \dots, y_n(t)]^\top$, we obtain the following bivirus dynamics for the meta-population network:

$$\dot{x}(t) = -x(t) + (I - X(t) - Y(t))Ax(t) \tag{2a}$$

$$\dot{y}(t) = -y(t) + (I - X(t) - Y(t))By(t), \tag{2b}$$

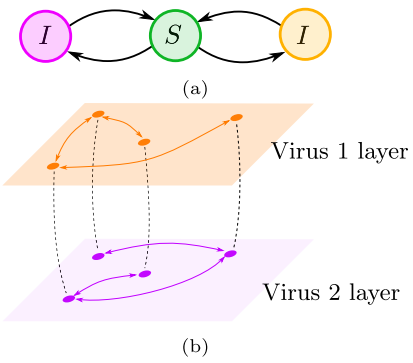

Fig. 1. Schematic of the compartment transitions and two-layer infection network. (a) Each individual exists in one of three health states: Susceptible (S, green), Infected with virus 1 (I, orange), or Infected with virus 2, (I, purple). Arrows represent possible transitions between compartments. (b) The two-layer network through which the viruses can spread between populations (nodes). Note that the edge sets of the two layers do not need to match, so that virus 1 can spread between two nodes but virus 2 cannot, and vice versa. (For interpretation of the references to color in this figure legend, the reader is referred to the web version of this article.)

where $X = \mathrm{diag}(x_1, \dots, x_n)$, and $Y = \mathrm{diag}(y_1, \dots, y_n)$. The system in Eq. (2) has state variable $(x(t), y(t))$, and is in fact a mean-field approximation of a coupled Markov process that captures the SIS bivirus contagion process [9,11,26]. Note that we have taken the recovery rates for both viruses to be equal to unity for every population for the purposes of clarity. Importantly, this can actually be done without loss of generality when examining the stability properties of equilibria for the bivirus system (see [12, Lemma 3.7]). It is known from [11, Lemma 8] that Δ is a positive invariant set for the bivirus dynamics in Eq. (2). Given that x_i and y_i represent the fraction of population i infected with virus 1 and virus 2, respectively, we naturally consider Eq. (2) exclusively in Δ, so that $x_i(t)$ and $y_i(t)$ retain their physical meaning in the context of the model for all $t \geq 0$. We have the following remark.

Remark 1. Our paper considers Eq. (2) in the context of a meta-population model. In some literature [9,11], node i is taken to be a single individual, and x_i and y_i are the probabilities that individual i is infected with virus 1 and virus 2, respectively. In other literature [8], the nodes may represent groups of individuals split according to some demographic characteristics, e.g., male or female. Depending on the modeling context, the diagonal entries of A and B may be zero (e.g., an individual cannot infect themselves), or A and B may be constrained to have the same zero and nonzero entry pattern (the two layers have the same topologies, but possibly different edge weights). Irrespective of the context, the dynamics are as given in Eq. (2), and the results in this paper are *equally applicable* to various alternative physical/epidemiological interpretations of the model. This is because all of the aforementioned modeling frameworks are equivalent, see [27].

We place the following standing assumption on the network topology.

Assumption 1. The matrices A and B are irreducible, which is equivalent to both layers of $\mathcal{G}$ being, separately, strongly connected.

In the epidemiological context, this implies that there exists an infection pathway for the virus from any node to any other node. Strong connectivity is a standard assumption for Eq. (2) (see [11,12,19]) and sometimes assumed without explicit statement [9] or is inherent from the problem formulation [8].

The second standing assumption of the paper is now stated, and as we will explain below, is in place due to our interest in survival-of-the-fittest outcomes.

Assumption 2. There holds $\rho(A) > 1$ and $\rho(B) > 1$.

There is always the healthy equilibrium $(x = \mathbf{0}_n, y = \mathbf{0}_n)$, where both viruses are extinct, and under Assumption 2, it is an unstable equilibrium (in fact, a repeller such that all trajectories starting in its neighborhood move away from it) [11]. With irreducible A and B, there can be at most three *types* of equilibria. There can be two "survival-of-the-fittest" equilibria $(\bar{x}, \mathbf{0}_n)$ and $(\mathbf{0}_n, \bar{y})$, where $\mathbf{0}_n < \bar{x} < \mathbf{1}_n$ and $\mathbf{0}_n < \bar{y} < \mathbf{1}_n$ [11] (also referred to as boundary equilibria elsewhere in the literature [12]). Assumption 2 is relevant here: the necessary and sufficient conditions for $(\bar{x}, \mathbf{0}_n)$ and $(\mathbf{0}_n, \bar{y})$ to exist are $\rho(A) > 1$ and $\rho(B) > 1$, respectively, see [11, Theorem 2 and Theorem 3]. Moreover, $\bar{x}$ and $\bar{y}$ correspond to the unique endemic equilibrium of the classical SIS model considering only virus 1 and only virus 2, respectively [11,20,28,29]. These two separate single virus systems are given by

$$\dot{x}(t) = -x(t) + (I - X(t))Ax(t), \tag{3a}$$

$$\dot{y}(t) = -y(t) + (I - Y(t))By(t). \tag{3b}$$

In the sequel, we provide a brief summary of the single virus system dynamics, including results useful for our theoretical analysis. The third type of equilibrium involves *coexistence* of both viruses, and any such equilibrium $(\tilde{x}, \tilde{y})$ must necessarily satisfy $\tilde{x} > \mathbf{0}_n$, $\tilde{y} > \mathbf{0}_n$ and $\tilde{x} + \tilde{y} < \mathbf{1}_n$ [12]. Assumption 2 is the necessary condition for existence of a coexistence equilibrium, but it is not sufficient [12]. Bivirus systems can have a unique coexistence equilibrium which can be stable or unstable (uniqueness has only been established for $n \leq 3$) [8,12], or multiple (including an infinite number) [11,12,24,30], or none [8,10,12].

Next, we remark that recent results show that for a 'generic' bivirus network, convergence to a stable equilibrium (of which there can be multiple) occurs for 'almost all' initial conditions [12,22] (see [12,22] for technical definitions of 'generic' and 'almost all'). Hence, the key question is as follows: to which equilibrium does convergence occur? We are now ready to formulate the problem to be studied, which deals with bivirus networks with at least two *stable* attractive equilibria.

Problem formulation. In this paper, we study scenarios where either of the viruses can win the survival-of-the-fittest battle, under Assumptions 1 and 2. Such scenarios are uncovered by examining the stability properties of the two equilibria $(\bar{x}, \mathbf{0}_n)$ and $(\mathbf{0}_n, \bar{y})$ for the network dynamics in Eq. (2). Namely, we seek to study bivirus networks with conditions on A and B that ensure both $(\bar{x}, \mathbf{0}_n)$ and $(\mathbf{0}_n, \bar{y})$ are locally exponentially stable. In such a scenario, there exist open sets $U \in \mathrm{Int}(\Delta)$ and $W \in \mathrm{Int}(\Delta)$, with non-zero Lebesgue measure and $U \cap W = \emptyset$, such that $\lim_{t\to\infty}(x(t), y(t)) = (\bar{x}, \mathbf{0}_n)$ for all $(x(0), y(0)) \in U$ and $\lim_{t\to\infty}(x(t), y(t)) = (\mathbf{0}_n, \bar{y})$ for all $(x(0), y(0)) \in W$. In context, the winner of a survival-of-the-fittest battle depends on the initial conditions.

The local exponential stability and instability of $(\bar{x}, \mathbf{0}_n)$ and $(\mathbf{0}_n, \bar{y})$ can be characterized by analysis of the Jacobian of the right hand side of Eq. (2), evaluated at the two equilibria. Let $\bar{X} = \mathrm{diag}(\bar{x}_1, \dots, \bar{x}_n)$ and $\bar{Y} = \mathrm{diag}(\bar{y}_1, \dots, \bar{y}_n)$. We recall the following result of [12, Theorem 3.10].

Proposition 1. *Consider Eq. (2) under Assumption 1. Then the following hold:*

1. *The equilibrium $(\bar{x}, \mathbf{0}_n)$ is locally exponentially stable if and only if $\rho((I - \bar{X})B) < 1$.*
2. *The equilibrium $(\mathbf{0}_n, \bar{y})$ is locally exponentially stable if and only if $\rho((I - \bar{Y})A) < 1$.*

The equilibria $(\bar{x}, \mathbf{0}_n)$ and $(\mathbf{0}_n, \bar{y})$ are unstable if the corresponding inequality in the proposition are reversed. Notice that the inequalities in Proposition 1 involve $\bar{X}$ and $\bar{Y}$ which are nonlinear functions of A and B, respectively. In other words, $\rho((I - \bar{X})B)$ depends on B explicitly and A implicitly, and hence the stability property of $(\bar{x}, \mathbf{0}_n)$ is tied to the complex interplay between the A and B matrices, or equivalently, between the edge set and edge weights of the two layers.

The same is true for $(\mathbf{0}_n, \bar{y})$. However, if one were provided A and B, it is straightforward to check if the conditions in Proposition 1 are met, since there are iterative algorithms to compute $\bar{x}$ and $\bar{y}$, e.g., [31, Theorem 4.3] or [32, Theorem 5].

The two statements in Proposition 1, depending on whether or not they are fulfilled, spawn three possibilities with respect to the dynamical behavior that system Eq. (2) exhibits.

Scenario 1: if the condition in statement 1 is satisfied, but the condition in statement 2 is not satisfied, then $(\bar{x}, \mathbf{0}_n)$ is locally exponentially stable and $(\mathbf{0}_n, \bar{y})$) is unstable. Parameter-based conditions, involving A and B, guaranteeing the same have been identified in [8–12,18,20]. In this scenario, for all initial conditions in $\mathrm{Int}(\Delta)$, virus 2 can never win a survival-of-the-fittest battle, while virus 1 can win such a battle [8–12,18,20], or both viruses coexist at a locally stable coexistence equilibrium [24].

Scenario 2: if both the conditions in statements 1 and 2 are violated, then both $(\bar{x}, \mathbf{0}_n)$ and $(\mathbf{0}_n, \bar{y})$) are unstable, and hence convergence must occur to a coexistence equilibrium (which may or may not be unique [24,30]). Thus, no virus can win a survival-of-the-fittest battle. Parameter-based conditions guaranteeing simultaneous instability of both $(\bar{x}, \mathbf{0}_n)$ and $(\mathbf{0}_n, \bar{y})$ have been provided in [8,9,20]. To wit, it is straightforward to identify conditions on A and B that cover the two scenarios discussed so far, and to generate numerical examples for such networks with arbitrary n nodes.

Scenario 3: if the conditions in statements 1 and 2 are simultaneously satisfied, then both $(\bar{x}, \mathbf{0}_n)$ and $(\mathbf{0}_n, \bar{y})$ are locally exponentially stable. Furthermore, in such a situation, there exists an unstable coexistence equilibrium [24, Corollary 3.9]. In this final scenario, multiple survival-of-the-fittest outcomes with either virus winning can occur, depending on the initial state.

In contrast to the stability configurations discussed previously, existence and design of network topology to ensure both $(\bar{x}, \mathbf{0}_n)$ and $(\mathbf{0}_n, \bar{y})$ are simultaneously locally stable has, to the best of our knowledge, not been addressed in the literature. The challenges involved are as follows: First, proving the *existence* of a bivirus system, with an arbitrary number of nodes, satisfying the conditions in Proposition 1 has remained an elusive challenge. This is primarily because it is not automatically guaranteed that there exist A and B which satisfy *one* let alone both of conditions for local exponential stability given above. Second, no systematic methods have been developed for designing bivirus networks to satisfy this third scenario. *The goal of the paper is to develop a systematic procedure to design bivirus networks, with dynamics as in Eq. (2), such that both $(\bar{x}, \mathbf{0}_n)$ and $(\mathbf{0}_n, \bar{y})$ are simultaneously locally exponentially stable.*

3. Main results

The main theoretical results of this work are presented in two parts. First, we present an existence result which states that given almost any A matrix, a corresponding B matrix can be found to satisfy the desired stability condition. Second, we detail the four-step procedure for finding such a B matrix, given a A matrix.

3.1. Preliminaries on matrix theory and single virus SIS systems

We recall relevant results from matrix theory and properties of the single SIS network model, required for deriving the main theoretical results. We say that a square matrix A is a nonnegative (positive) matrix if all of its entries are nonnegative (positive). A nonnegative matrix A is irreducible if and only if whenever $y = Ax$, with $x \geq \mathbf{0}_n$, y always has a nonzero entry in at least one position where x has a zero entry. If A is nonnegative and irreducible, then by the Perron–Frobenius Theorem [33], $\sigma(A) = \rho(A)$ is a simple eigenvalue, and we call it the Perron–Frobenius eigenvalue of A. The associated eigenvector can be chosen to have all positive entries, and up to a scaling, there is no other eigenvector with this property. We say that A is a Metzler matrix if all of its off-diagonal entries are nonnegative. By applying the Perron–Frobenius Theorem [33] to a Metzler and irreducible A, similar conclusions on $\sigma(A)$ and the corresponding eigenvector can be drawn. A square matrix A is an M-matrix if $-A$ is Metzler and all eigenvalues of A have positive real parts except for any at the origin. If A has eigenvalues with strictly positive real parts, we call it a nonsingular M-matrix, and a singular M-matrix otherwise [33].

Some properties of M-matrices and Metzler matrices, relevant to our theoretical results, are detailed as follows:

1. For a (singular) M-matrix F, and any positive diagonal D, DF is also a (singular) M-matrix.
2. Let F be an irreducible singular M-matrix. Then, for any nonnegative nonzero diagonal D, $F+D$ is an irreducible nonsingular M-matrix.
3. Let B be nonnegative irreducible and D be positive diagonal. Then for the Metzler matrix $-D+B$, there holds (i) $\sigma(-D+B) > 0 \Leftrightarrow \rho(D^{-1}B) > 1$, (ii) $\sigma(-D+B) = 0 \Leftrightarrow \rho(D^{-1}B) = 1$ and (iii) $\sigma(-D+B) < 0 \Leftrightarrow \rho(D^{-1}B) < 1$.
4. For an irreducible nonnegative matrix B and a positive diagonal matrix D with $d_{ii} < 1\ \forall i$, there holds $\rho(B) > \rho((I-D)B)$ and $\rho(B) > \rho(DB)$.
5. For a nonsingular irreducible M-matrix F, F^{-1} is a positive matrix.

The first two results are easily proved from the property that all the principal minors of an M-matrix are positive in the nonsingular case and nonnegative in the singular case, see [34, Theorem 4.31] and [25, Chapter 6, Theorem 2.3 and Theorem 4.6]. The third result is due to [11, Proposition 1]. The fourth is a consequence of [25, Chapter 2, Corollary 1.5(b)] and the irreducibility of both $(I-D)B$ and DB, which sum to B. The fifth is a consequence of [25, Chapter 6, Theorem 2.7].

We now recall results for the single virus system in Eq. (3a), but obviously the same results will hold for Eq. (3b). The limiting behavior of Eq. (3a) can be fully characterized by $\rho(A)$, see e.g., [29,31,35]. Specifically, if $\rho(A) \leq 1$, then $\lim_{t\to\infty} x(t) = \mathbf{0}_n$ for all $x(0) \in [0,1]^n$. We call $\mathbf{0}_n$ the healthy equilibrium. If $\rho(A) > 1$, then $\lim_{t\to\infty} x(t) = \bar{x}$ for all $x(0) \in [0,1]^n \setminus \{\mathbf{0}_n\}$, where $\mathbf{0}_n < \bar{x} < \mathbf{1}_n$ is the unique non-zero (endemic) equilibrium which is exponentially stable. Note that the equilibrium equation yields:

$$[-I + (I - \bar{X})A]\bar{x} = \mathbf{0}_n, \tag{4}$$

with $\bar{X} = \mathrm{diag}(\bar{x})$. The following result characterizes properties of the matrix on the left of Eq. (4).

Lemma 1. *Consider the single virus system in Eq. (3a), and suppose that $\rho(A) > 1$ and A is irreducible. With respect to Eq. (4), the following hold:*

1. *The matrix $-I + (I - \bar{X})A$ is a singular irreducible Metzler matrix;*
2. *$\sigma(-I+(I-\bar{X})A) = 0$ is a simple eigenvalue with an associated unique (up to scaling) left eigenvector $u^\top$ and right eigenvector $\bar{x}$, with all entries positive, i.e. $u^\top \gg \mathbf{0}_n$ and $\bar{x} \gg \mathbf{0}_n$.*

Proof. Regarding the first statement, observe that $\mathbf{0}_n \ll \bar{x} \ll \mathbf{1}_n$ guarantees that $(I-\bar{X})$ is a positive diagonal matrix, and hence $(I-\bar{X})A$ is irreducible precisely when A is irreducible. It is also nonnegative. Thus, $-I + (I - \bar{X})A$ is an irreducible Metzler matrix. Eq. (4) implies that $\bar{x}$ is a null vector of the matrix $-I + (I - \bar{X})A$, which accordingly is a singular matrix. Regarding the second statement, the conclusions immediately follow by viewing Eq. (4) in light of the properties of Metzler matrices detailed above. □

3.2. Existence of two stable survival equilibria

We now present the main theoretical result of this paper, showing that given almost any A matrix, one can find a B matrix (with $\rho(B) >$

1) such that the two spectral radius inequalities in Proposition 1 are satisfied.

Given A with $\rho(A) > 1$, let $u^\top$ and $\bar{x}$ be the eigenvectors stated in Lemma 1, normalized to satisfy $u^\top \bar{x} = 1$. Let B' be any other nonnegative and irreducible matrix such that

$$[I - (I - \bar{X})B']\bar{x} = \mathbf{0}_n, \tag{5}$$

which similarly implies that $\bar{x}$ is a positive right eigenvector for $-I + (I - \bar{X})B'$ associated to the simple eigenvalue at the origin. That such a B' exists and indeed has further properties yet to be stated will be demonstrated subsequently. Let $v^\top$ be the associated left eigenvector, normalized to satisfy $v^\top \bar{x} = 1$. Notice that our definition of B' implies that A and B' define the infection matrix for two separate single virus systems in Eqs. (3a) and (3b) that have the same endemic equilibrium.

We further require that u and v be linearly independent, and this can be straightforwardly achieved by selecting an appropriate B' when given A. Indeed, we present Lemma 2 in the sequel, showing a procedure to select B', when given A, to ensure the linear independence of u and v. The main result follows, with proof in Appendix.

Theorem 1. *Suppose that A and B' are irreducible nonnegative matrices, with $\rho(A) > 1$ and $\rho(B') > 1$, that satisfy Eqs. (4) and (5), respectively. Suppose further that $u^\top$ and $v^\top$, as defined above, are linearly independent. Then there exists $\delta x \in \mathbb{R}^n$ with arbitrarily small Euclidean norm $|\delta x|$ and satisfying*

$$u^\top[\bar{X}(I - \bar{X})^{-1}]\delta x > 0 \tag{6}$$

$$v^\top[\bar{X}(I - \bar{X})^{-1}]\delta x < 0. \tag{7}$$

Furthermore, there exists $\delta B \in \mathbb{R}^{n\times n}$ such that $B' + \delta B$ is an irreducible nonnegative matrix, and δB also satisfies

$$\delta B\bar{x} = [(I - \bar{X})^{-2} - B']\delta x. \tag{8}$$

Then, with $B := B' + \delta B$, for the bivirus network in Eq. (2), both the survival-of-the-fittest equilibria $(\bar{x}, \mathbf{0}_n)$ and $(\mathbf{0}_n, \bar{y})$ are locally exponentially stable, and $\bar{y} = \bar{x} + \delta x + o(|\delta x|)$, where $o(|\delta x|)$ is a vector with norm of order $|\delta x|^2$.

Provided δx and δB are sufficiently small, the resulting bivirus network in Eq. (2) is such that either virus 1 or virus 2 may win a survival-of-the-fittest battle, depending on whether the initial states $(x(0), y(0))$ are in the region of attraction for $(\bar{x}, \mathbf{0}_n)$ or $(\mathbf{0}_n, \bar{y})$, respectively. Our result does not exclude other limiting behavior, such as converging to a coexistence equilibrium where every population i has individuals infected with virus 1 and virus 2. This is because the regions of attraction for $(\bar{x}, \mathbf{0}_n)$ and $(\mathbf{0}_n, \bar{y})$ together cannot cover all of $\mathrm{Int}(\Delta)$ [36], since there will be points in $\mathrm{Int}(\Delta)$ which are on the boundary of one or both regions of attraction (and thus cannot be part of the region). Indeed, there exist numerical examples where both $(\bar{x}, \mathbf{0}_n)$ and $(\mathbf{0}_n, \bar{y})$ locally exponentially stable, and there are also multiple locally exponentially stable coexistence equilibria [24].

3.3. Systematic construction procedure

To begin, we provide a specific method for constructing a suitable B', with proof given in Appendix. Let e_i be the ith basis vector, with 1 in the ith entry and 0 elsewhere.

Lemma 2. *Let A be an irreducible nonnegative matrix fulfilling Eq. (4) for some $\bar{x}$ such that $\mathbf{1}_n > \bar{x} > \mathbf{0}_n$. For a fixed but arbitrary $i \in \mathcal{V}$, let $z^\top \neq \mathbf{0}_n$ be chosen to satisfy $z^\top \bar{x} = 0$ and the jth entry $z_j < 0$ only if $a_{ij} > 0$. Then, there exists a sufficiently small ϵ such that $B' := A + \epsilon e_i z^\top$ is an irreducible nonnegative matrix. Moreover, B' fulfills the conditions in the hypothesis of Theorem 1: $\rho(B') > 1$, Eq. (5) is satisfied, and u and v are linearly independent.*

A procedure to systematically construct a bivirus network according to Theorem 1 is now presented.

Step 1. Consistent with Theorem 1, we begin by assuming that we are given an irreducible nonnegative matrix A with spectral radius greater than 1. Construct the matrix $B' = A + \epsilon e_i z^\top$ according to Lemma 2.

Step 2. With $u^\top$ and $v^\top$ as defined in Section 3.2, set $F = (I - \bar{X})^{-2} - B'$ and $\tilde{u}^\top = u^\top \bar{X}(I - \bar{X})^{-1}F^{-1}$ and $\tilde{v}^\top = v^\top \bar{X}(I - \bar{X})^{-1}F^{-1}$. Note that F is invertible and F^{-1} is a positive matrix, as detailed in Appendix. Select two integers j and k for which $\tilde{u}_j/\tilde{u}_k > \tilde{v}_j/\tilde{v}_k$. This is possible since $u^\top$ and $v^\top$ (and thus $\tilde{u}^\top$ and $\tilde{v}^\top$ also) are linearly independent. Select $\alpha > 0$ to satisfy

$$\alpha\tilde{u}_j/\tilde{u}_k > 1 > \alpha\tilde{v}_j/\tilde{v}_k,$$

noting that such an α can always be found. Identify one positive entry in each of the jth row and kth row of B', say b'_{jp} and b'_{kq}. Set $\beta \in (0, b'_{kq}\bar{x}_q)$. Finally, define the vector $s \in \mathbb{R}^n$ which has zeros in every entry except $s_k = -\beta$ and $s_j = \alpha\beta$. Compute $\delta x = F^{-1}s$.

Step 3. To obtain δB, set all of its entries to be equal to zero, except that $\delta b_{kq} = -\beta/\bar{x}_q$ and $\delta b_{jp} = \alpha\beta/\bar{x}_p$. Then, set $B = B' + \delta B$.

Step 4. (If necessary). Check that the resulting B satisfies the necessary and sufficient condition for local stability outlined in Proposition 1, and if not, iterate Step 1–3 with different choices of $z^\top$, ϵ, α, and β. The theoretical analysis uses arguments centered on perturbation methods (see Appendix), and the δx and δB must be sufficiently small. The design choices of the construction method are $z^\top$, ϵ, α, and β, and hence one may need to adjust/tune these values in order to obtain a suitable B. Nonetheless, existence of such B is guaranteed by Theorem 1.

With $z^\top$, ϵ, α, and β as the design choices, there are numerous potential options which give rise to different suitable B. For instance, since $\bar{x} > \mathbf{0}_n$, z must have at least one positive and one negative entry in order to satisfy $z^\top \bar{x} = 0$, and so one straightforward implementation is to set $z_k = 1$ and $z_j = -\bar{x}_k/\bar{x}_j$, for arbitrary k, j. For the selected index j, we need $\epsilon < \min_{\{l\in\mathcal{V}:a_{lj}>0\}} a_{lj}/z_j$ to ensure that B' is nonnegative. Then, B' is equal to A except for the following entries: for the particular choice of e_i, $b'_{im} = a_{im} + \epsilon z_m$ for any $z_m \neq 0$. Next, B is equal to B' except the entries $b_{kq} = b'_{kq} - \beta/\bar{x}_q$ and $b'_{jp} = a_{jp} + \alpha\beta/\bar{x}_p$ for the indices j, k, p, q identified in Step 2.

If A is a positive matrix, corresponding to an all-to-all connected virus 1 layer, then a more straightforward approach can be taken. We set $B' = A + \epsilon\mathbf{1}_n z^\top$, with $z^\top \bar{x} = 0$ and ϵ sufficiently small to guarantee B' is a positive matrix. Then, solve Eqs. (6) and (7) for δx using standard linear programming methods. Next, compute a solution δB for Eq. (8) and apply a scaling constant to decrease the entries of δB to ensure that $B = B' + \delta B$ remains a positive matrix. The challenge occurs when A and B' are not positive matrices, because any δB satisfying Eq. (8) must have both positive and negative entries. This can be problematic if we obtain a solution δB that has a negative entry where B' has a zero entry but we also require B to be nonnegative irreducible. The above four-step procedure resolves this issue, by producing a δB whose single negative entry is in the same position corresponding to a positive entry in B', and the former is smaller in magnitude than the latter.

To apply the four-step construction procedure, one requires knowledge of the infection matrix A, from which one can compute the endemic equilibrium $\bar{x}$ associated with Eq. (3a) (see below Proposition 1). It is important to stress that only knowledge of the single virus system is needed, as opposed to knowledge of any bivirus system. From knowledge of A and $\bar{x}$, one constructs a suitable B', and then computes δx and δB as necessary. The next two remarks provide additional context for our results.

Remark 2. Our analysis and results assume that a starting A matrix is given associated with a strongly connected graph layer in the two-layer network. Theorem 1 guarantees the existence of an irreducible B matrix (and thus its associated graph is strongly connected) such that both survival-of-the-fittest equilibria of the resulting bivirus system are

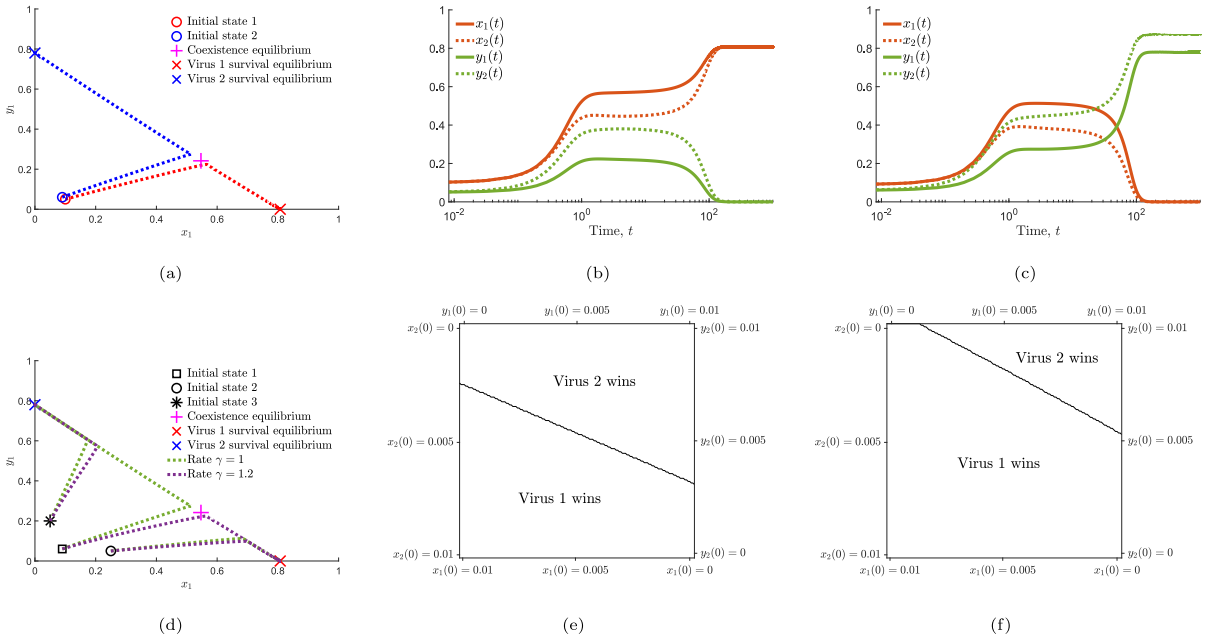

Fig. 2. The dynamics of the two-node case study of Eq. (2). In (a), the trajectories $(x_1(t), y_1(t))$ are shown for two different initial states (red and blue); virus 1 and virus 2 win the survival-of-the-fittest battle in the red and blue trajectories, respectively. In (b) and (c), the time evolution of $(x(t), y(t))$ is shown for the red and blue trajectories in (a), respectively. In (d), we show the trajectories $(x_1(t), y_1(t))$ for virus 1 and virus 2 of the same speed (green, $\gamma = 1$) and virus 1 that is 1.2 times faster relative to virus 2 (purple, $\gamma = 1.2$), for different initial states. The winning virus for different initial states is recorded when (e) virus 1 and virus 2 are the same speed and (f) when virus 1 is faster than virus 2, with $\gamma = 1.2$. Note the line where the boundaries of the two regions meet forms part of the stable manifold of the unstable coexistence equilibrium. (For interpretation of the references to color in this figure legend, the reader is referred to the web version of this article.)

locally stable. Additionally, Lemma 2 and the four-step construction method present a method for constructing an irreducible B, given an irreducible A. In other words, our results in Section 3 guarantee that if A meets Assumption 1, then any resulting B we obtain also satisfies the assumption. This is the extent to which our results depend on the structure of the graphs.

Remark 3. Ref. [8] provided a comprehensive analysis of a specific $n = 3$ network, corresponding to certain entries of A and B having being fixed at zero. This included identifying conditions where the winning virus in a survival-of-the-fittest battle depended on the initial states. We do not impose constraints on the network structure, whether for the $n = 3$ case or any other value of n. Consequently, even for the $n = 3$ case, the findings of the present paper are novel. Our results are applicable for n node networks (with n arbitrary but finite). We also note that due to the constraints on A and B, any coexistence equilibrium in the $n = 3$ network in Ref. [8] must be unique. This contrasts our recent findings (and consistent with the results of this paper), where it is possible to have multiple coexistence equilibria for general network structures [24].

4. Simulation case studies

We now present two case studies to illustrate the procedure and the different survival-of-the-fittest outcomes. Full code is available at https://github.com/lepamacka/bivirus_code and https://github.com/mengbin-ye/bivirus.

4.1. Two-node case study

We consider a setting involving a two-node network, with each layer of the graph being complete. More specifically, we used the following matrices:

$$A = \begin{bmatrix} 3.2 & 2 \\ 2 & 3.2 \end{bmatrix}, \quad B = \begin{bmatrix} 4.2 & 0.312 \\ 6.1318 & 2.2 \end{bmatrix}. \tag{9}$$

Note that for this simulation, and consistent with the assumptions in Theorem 1 and Section 3.3, the matrix A is given; the matrix B is obtained using the 4-step procedure that we have outlined in Section 3.3. The two single virus systems defined using the A and B above (see Eqs. (3a) and (3b)) have the following two endemic equilibria $\bar{x} = [0.8077, 0.8077]^\top$ and $\bar{y} = [0.7801, 0.8699]^\top$, respectively. These define two survival-of-the-fittest equilibria $(\bar{x}, \mathbf{0}_n)$ and $(\mathbf{0}_n, \bar{y})$ for the bivirus system in Eq. (2). We then obtain $\rho((I - \bar{Y})A) = 0.9276$ and $\rho((I - \bar{X})B) = 0.9436$, which establishes that each survival-of-the-fittest equilibrium is locally exponentially stable, due to Proposition 1. For $n = 2$, one can analytically compute coexistence equilibria, see [12]. We used Maple to analytically identify a unique coexistence equilibrium $(\tilde{x}, \tilde{y})$:

$$\tilde{x} = \begin{bmatrix} 0.5467 & 0.4180 \end{bmatrix}^\top, \ \tilde{y} = \begin{bmatrix} 0.2418 & 0.4101 \end{bmatrix}^\top. \tag{10}$$

The Jacobian matrix of Eq. (2) at this coexistence equilibrium has three negative real eigenvalues of -5.4373, -3.8924 and -0.7507 and one unstable eigenvalue of 0.0321 (see [12,22] for expressions of the Jacobian matrix).

Fig. 2(a) shows the phase portrait for two initial states in $\mathrm{Int}(\Delta)$ that are close together: Initial state 1, $x(0) = [0.1, 0.1]^\top$ and $y(0) = [0.05, 0.05]^\top$, and Initial state 2, $x(0) = [0.09, 0.09]^\top$ and $y(0) = [0.06, 0.06]^\top$. Different survival-of-the-fittest outcomes occur, with either virus 1 (blue) or virus 2 (red) winning. Figs. 2(b) and 2(c) show the time evolution of the blue and red trajectories in Fig. 2(a), respectively. It is notable that there is a rapid initial transient that takes the system to a point very close to a curve that connects $(\bar{x}, \mathbf{0}_n)$ to $(\mathbf{0}_n, \bar{y})$ and passes through the unstable coexistence equilibrium (magenta cross), followed by a slower convergence to the two survival equilibria.

Separating the time-scales of the viruses can change the shape of the regions of attraction for $(\bar{x}, \mathbf{0}_n)$ and $(\mathbf{0}_n, \bar{y})$, but the local exponential stability property is unchanged, and thus both regions will always have non-zero Lebesgue measure. Time-scale separation can be achieved by introducing a parameter $\gamma > 0$ and modifying Eq. (2a) to be

$$\dot{x}(t) = \gamma\Big(-x(t) + (I - X(t) - Y(t))Ax(t)\Big). \tag{11}$$

Adjusting γ allows study of scenarios of interest where virus 1 has much faster or slower dynamics relative to virus 2. Fig. 2(d) shows the trajectories for the two viruses having the same speed (green) and virus 1 being faster than virus 2 (purple, $\gamma = 1.2$). We set "Initial state 1" (square symbol) to be $x(0) = [0.09, 0.09]^\top$ and $y(0) = [0.06, 0.06]^\top$, "Initial state 2" (circle symbol) as $x(0) = [0.25, 0.25]^\top$ and $y(0) = [0.05, 0.05]^\top$, and "Initial state 3" ($\ast$ symbol) as $x(0) = [0.05, 0.05]^\top$ and $y(0) = [0.2, 0.2]^\top$. The unique coexistence equilibrium (magenta cross) remains unchanged for any positive γ. Thus, from the same initial condition, the virus that survives may depend on the relative speeds of the two viruses, but there are always two nontrivial regions of attraction for the two stable equilibria.

In Fig. 2(e), we create a 150×150 grid of initial states, imposing a constraint that $x_i(0) + y_i(0) = 0.01$ for $i = 1, 2$. For each point on this grid, we simulated the system over a large time window and recorded the particular equilibrium point reached. The figure thus divides the phase plane into two regions of attraction, for initial states that resulted in virus 1 or virus 2 winning the survival-of-the-fittest battle. Fig. 2(f) is generated using the exact same procedure as Fig. 2(e), except we change the timescale for virus 1 by setting $\gamma = 1.2$, resulting in a marked shift in the regions of attraction. It appears that as the dynamics of one virus becomes faster, the region of attraction increases in size, which accords with intuition.

It is known that the region of attraction for an equilibrium forms an open set [36], and in our case study there are two locally stable equilibria (the two survival-of-the-fittest equilibria) and two unstable equilibria (the healthy equilibrium and the coexistence equilibrium). Thus, the boundaries of the regions of attraction for $(\bar{x}, \mathbf{0}_n)$ and $(\mathbf{0}_n, \bar{y})$ do not belong to the region of attraction of either, and if the system is initialized at a common point of the two boundaries, then necessarily the trajectories do not converge to either stable equilibrium. In fact, the common boundary of the two regions of attraction forms the stable manifold of the coexistence equilibrium $(\tilde{x}, \tilde{y})$, which has zero Lebesgue measure [36]. Initial states on this manifold would lead to convergence to $(\tilde{x}, \tilde{y})$, providing a third outcome of the battle, namely coexistence, which is unlikely to be encountered in practice but is not impossible. Certain trajectories may appear to converge to the unstable equilibrium, but after some time end up moving on to one of the survival-of-the-fittest equilibria.

4.2. Real-world network case study

In this section, we present a case study involving a real-world network topology to demonstrate that our procedure works for large-scale real world networks as well, and not just a small 2-node example as above. We consider a mobility network reported in Ref. [37], capturing commuting patterns for people between $n = 107$ provinces in Italy. The original network $\bar{\mathcal{G}}$, with associated adjacency matrix $\bar{A}$, is a complete directed graph, i.e., $\bar{A}$ is a positive matrix but it is not symmetric. Due to differences in commuting patterns, journeys between some provinces were highly frequent, whereas journeys between some other provinces were virtually nonexistent save for a small number of individuals, so the largest and smallest entries of $\bar{A}$ differed by several orders of magnitude. For computational convenience, we first normalize this matrix so that the row sums are equal to 2, i.e. $\bar{A}\mathbf{1}_n = 2\mathbf{1}_n$. Then, we obtain the matrix A by setting each entry as $a_{ij} = \bar{a}_{ij}$ if $\bar{a}_{ij} \geq \kappa$, and $a_{ij} = 0$ otherwise, where the scalar $\kappa > 0$ acts as a threshold. By using $\kappa = 5 \times 10^{-5}$, we obtained an A matrix that was nonnegative irreducible but not positive (and thus the graph associated with A is strongly connected but not complete). We normalized A to satisfy $A\mathbf{1}_n = 2\mathbf{1}_n$, and then set A to be the adjacency matrix associated with the network layer of virus 1.

We followed the systematic construction procedure outlined in Section 3.3 to obtain B, which we now briefly outline. First, note that $\bar{x} = 0.5\mathbf{1}_n$ due to our normalization. We selected the 48-th basis vector, i.e., $i = 48$ for the vector e_i. The vector z (of dimension 107) was a vector of zeros, except $z_{48} = 1$ and $z_{55} = -1$, and $\epsilon = 0.2346$. After following the four step construction procedure, we obtained $B = A$, with the exception that the following four entries were adjusted: $b_{48,48} = a_{48,48} + 0.2346$, $b_{48,55} = a_{48,55} - 0.2346$, $b_{48,69} = a_{48,69} - 0.0205$, $b_{55,100} = a_{55,100} + 5.0795 \times 10^{-4}$. It turns out that $\rho((I - \bar{Y})A) = 0.9999914$ and $\rho((I - \bar{X})B) = 0.9999964$, and hence $(\bar{x}, \mathbf{0}_n)$ and $(\mathbf{0}_n, \bar{y})$ are locally exponentially stable. The network is shown in Fig. 3(c), with the matrices A and B found in the online repository mentioned at the beginning of Section 4.

We consider two sets of initial conditions. We first sample p_i and q_i from a uniform distribution $(0, 1)$, for all $i \in \{1, \ldots, n\}$. For the first set of initial conditions, we set $x_i(0) = p_i/(p_i+q_i)$ and $y_i(0) = 0.1q_i/(p_i+q_i)$. This ensures that $x_i(0)+y_i(0) < 1$ as required, and the initial virus 1 infection level is ten times that of virus 2 at any node i. For the second set of initial conditions, we set $x_i(0) = p_i/(p_i + q_i)$ and $y_i(0) = 0.5q_i/(p_i + q_i)$. Hence, the initial virus 1 infection level is twice as large as that of virus 2 for any node i. Fig. 3(a) corresponds to the first set of initial conditions, where virus 1 emerges as the winner of the survival-of-the-fittest battle. In contrast, Fig. 3(b) corresponds to the second set of initial conditions, where virus 2 wins the battle. Interestingly, virus 2 is still able to win the survival-of-the-fittest battle, even if initial infection levels were on average twice as smaller for virus 2 compared to virus 1.

To summarize, in this section, we have demonstrated that the findings of this paper are applicable for not just small networks but also for real-world large-scale networks.

5. Conclusion

In summary, we explored a fundamental problem for competing epidemics spreading using the deterministic SIS bivirus network model. We provided a rigorous argument which established that for almost any A, there exists a B such that the pair of matrices (A, B) satisfied a certain necessary and sufficient condition under which the winner of a survival-of-the-fittest battle depends nontrivially on the initial state of the bivirus network. Then, we presented a systematic procedure to generate such a bivirus network, and studied three numerical examples. This paper significantly expands the known dynamical phenomena of the bivirus model, but should be considered as just a first important step for the epidemic modeling community to explore the diverse new outcomes that are now unlocked for competing epidemic spreading models. A key direction of our future work is to investigate models of three or more competing viruses (multivirus networks) [20], and to explore how the regions of attraction might change as a function of the relative speeds of the different virus dynamics.

CRediT authorship contribution statement

Mengbin Ye: Conceptualization, Formal analysis, Funding acquisition, Investigation, Methodology, Software, Visualization, Writing – original draft. **Brian D.O. Anderson:** Conceptualization, Formal analysis, Methodology, Writing – original draft. **Axel Janson:** Investigation, Methodology, Software, Validation, Visualization, Writing – review & editing. **Sebin Gracy:** Formal analysis, Methodology, Writing – original draft. **Karl H. Johansson:** Conceptualization, Funding acquisition, Methodology, Resources, Supervision, Writing – review & editing.

Declaration of competing interest

The authors declare the following financial interests/personal relationships which may be considered as potential competing interests: Mengbin Ye reports financial support was provided by Western Australia Department of Jobs Tourism Science and Innovation and the Australian Government (through the Office of National Intelligence). Sebin Gracy, Axel Janson, and Karl H. Johansson report that financial support was provided by Knut and Alice Wallenberg Foundation. Karl H. Johansson also reports financial support provided by Swedish Research Council, and by the Swedish Strategic Research Foundation.

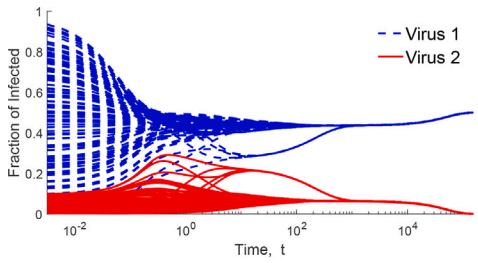

(a) Virus 1 wins

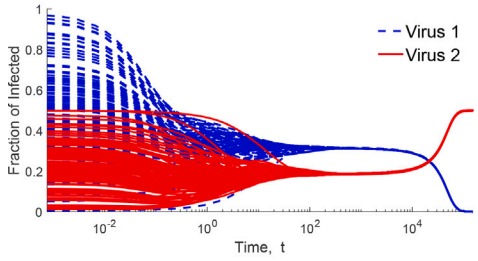

(b) Virus 2 wins

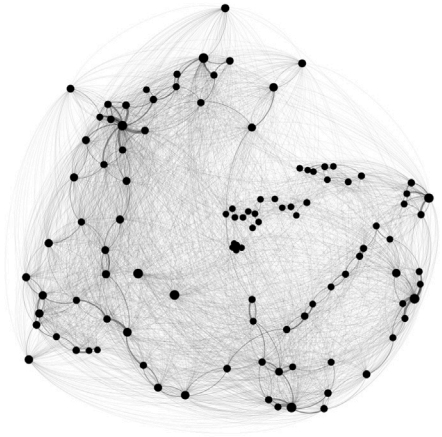

(c) Network of commuting patterns between Italian provinces

Fig. 3. The dynamics of the $n = 107$ example for a mobility network of Italian provinces (note the logarithmic scale of time, t, along the horizontal axis). In (a) and (b), the time evolution of $(x(t), y(t))$ shows two different initial states yielding two different survival-of-the-fittest outcomes. In (c), each of the 107 nodes represents a province in Italy, with edges denoting mobility pathways (darker edges indicate greater travel volume).

Data availability

All data and code are available in the online repositories referenced in the paper.

Appendix. Proof of Theorem 1 and Lemma 2

In order to prove the claim in Theorem 1, we need the following result on eigenvalue perturbation of a matrix, useful for the subsequent proof.

Lemma 3 (*[38, pg. 15.2, Fact 3]*). *Let $W \in \mathbb{R}^{n\times n}$ be a square matrix with left and right eigenvectors $a^\top, b$ corresponding to a real simple eigenvalue λ. Suppose that W is perturbed by a small amount $\delta W \in \mathbb{R}^{n\times n}$. Then to first order in δ, λ is perturbed by an amount $\delta\lambda$ given by $\delta\lambda = (a^\top \delta W b)/(a^\top b)$.*

Proof of Theorem 1. There are three key steps to the proof. Step 1 deals with the existence claims. Step 2 establishes that the relation Eq. (8) ensures that the bivirus system in Eq. (2), with infection matrices A and $B = B' + \delta B$, has the survival-of-the-fittest equilibrium associated with virus 2 at $(\mathbf{0}_n, \bar{x} + \delta x)$. Step 3 shows that the inequalities Eqs. (6) and (7) satisfied by δx cause both of the survival-of-the-fittest equilibria to be locally stable, exploiting inequality conditions in Proposition 1.

Before proceeding further, we highlight two important properties of equilibria for Eqs. (2) and (3) that underpin the perturbation approach. We are interested in the survival-of-the-fittest equilibrium at virus 2, viz. $(\mathbf{0}_n, \bar{y})$. The *stability* property of $(\mathbf{0}_n, \bar{y})$ must be studied via the bivirus system, Eq. (2). Indeed, this can be seen in Proposition 1, where the condition for stability of $(\mathbf{0}_n, \bar{y})$ involves both A and B (indirectly via $\bar{Y}$). On the other hand, the *location* of $(\mathbf{0}_n, \bar{y})$, and in particular the value of the entries of $\bar{y}$, can be studied using the single virus system Eq. (3b) because by definition $\dot{x} = x = \mathbf{0}_n$. Under Assumption 2, it is well known that the system Eq. (3b) has a unique endemic equilibrium $\bar{y}$ satisfying $\mathbf{0}_n < \bar{y} < \mathbf{1}_n$ and $\bar{y}$ is locally exponentially stable [35]. That is, the Jacobian matrix of the right-hand-side of Eq. (3b) is Hurwitz. Importantly, this means that $\bar{y}$ is a hyperbolic equilibrium, implying that the entries of $\bar{y}$ vary smoothly as a function of small perturbations to system parameters, in our case δB to obtain $B = B' + \delta B$. Essentially, no bifurcation (and thus changes to existence or number of equilibria) is possible for Eq. (3b) if δB is sufficiently small. The key challenge is to determine the location of $\bar{y}$ after perturbation (Step 2) and the stability of $(\mathbf{0}_n, \bar{y})$ (Step 3).

Step 1. Since $\mathbf{0}_n < \bar{x} < \mathbf{1}_n$, $I - \bar{X}$ is a positive diagonal matrix and its inverse exists. Since u, v are assumed to be linearly independent, the row vectors $u^\top[\bar{X}(I - \bar{X})^{-1}]$ and $v^\top[\bar{X}(I - \bar{X})^{-1}]$ are also linearly independent, and accordingly δx exists satisfying Eqs. (6) and (7) and its norm can be chosen arbitrarily by scaling. However, an additional requirement has to be met, viz. that Eq. (8) holds for some δB such that $B' + \delta B$ is irreducible and nonnegative. This is straightforward if B' is positive by scaling δB to have its entries sufficiently small in magnitude, but not when B' can have zero entries. To proceed, set $F = (I - X)^{-2} - B'$ and observe that $F = [(I - X)^{-2} - (I - X)^{-1}] + [(I - X)^{-1} - B']$, i.e. F is the sum of a diagonal positive matrix and an irreducible singular M-matrix. Hence it is an irreducible nonsingular M-matrix, and accordingly F^{-1} is a positive matrix. The two vectors $\tilde{u}^\top := u^\top \bar{X}(I - \bar{X})^{-1}F^{-1}$ and $\tilde{v}^\top := v^\top \bar{X}(I - \bar{X})^{-1}F^{-1}$ are then both positive and linearly independent. Let

$$s = \delta B \bar{x} \tag{A.1}$$

Finding δx and δB to satisfy Eqs. (6)–(8) is then equivalent to finding s and δB to satisfy Eq. (A.1) and

$$\tilde{u}^\top s > 0\,, \quad \text{and} \quad \tilde{v}^\top s < 0. \tag{A.2}$$

We shall now show that these requirements can be fulfilled by choosing just two of the entries of s to be nonzero, and likewise, just two of the entries of δB.

Because $\tilde{u}$ and $\tilde{v}$ are linearly independent, there is no nonzero μ for which $\tilde{u} = \mu\tilde{v}$. Thus, there must be two integers, say j and k, for which $\tilde{u}_j/\tilde{v}_j \neq \tilde{u}_k/\tilde{v}_k$. Without loss of generality (using renumbering if necessary) let us assume that $\tilde{u}_2/\tilde{v}_2 > \tilde{u}_1/\tilde{v}_1$, or equivalently, $\tilde{u}_2/\tilde{u}_1 > \tilde{v}_2/\tilde{v}_1$. Let $\alpha > 0$ be such that

$$\alpha\tilde{u}_2/\tilde{u}_1 > 1 > \alpha\tilde{v}_2/\tilde{v}_1 \tag{A.3}$$

Let $\beta > 0$ be a constant to be specified below, and choose $s = [-\beta, \alpha\beta, 0, \ldots, 0]^\top$. Using Eq. (A.3), it is immediate that Eq. (A.2) is satisfied. Now to specify δB, observe that the irreducibility of B' guarantees that at least one entry of the first row and one entry of the

second row are positive, say b'_{1i} and b'_{2j}. (They may or may not be in the same column.) Choose β such that $0 < \beta < b'_{1i}\bar{x}_i$, and set all entries of δB to zero except that

$$\delta b_{1i} = -\beta/\bar{x}_i \tag{A.4}$$

$$\delta b_{2j} = \alpha\beta/\bar{x}_j \tag{A.5}$$

These two definitions ensure that $s = \delta B\bar{x}$ as required, that $B' + \delta B$ is a nonnegative matrix, and that it is also irreducible since it has the same zero entries as B'. To summarize, setting δB using Eqs. (A.4) and (A.5) ensures that $B'+\delta B$ is a nonnegative irreducible matrix, while we select the specific form of s with first and second entry equal to $-\beta$ and $\alpha\beta$ to ensure that Eq. (A.2) is satisfied for the particular choice of δB.

Step 2. We first remark that, for the given A and our selected $B = B' + \delta B$, the two survival-of-the-fittest equilibria always exist. This is because $\rho(A) > 1$ and $\rho(B') > 1$ by hypothesis, each single virus endemic equilibrium is hyperbolic, and δB is small. The main challenge of this step is to establish that the two equilibria are located at $(\bar{x}, \mathbf{0}_n)$ and $(\mathbf{0}_n, \bar{y})$ with $\bar{y} = \bar{x} + \delta x + o(|\delta x|)$, where the notation $o(|\delta x|)$ refers to a vector with Euclidean norm of order higher than $|\delta x|$. Since Eq. (4) holds, the claim for $(\bar{x}, \mathbf{0}_n)$ is immediate. Put another way, $\bar{x}$ is determined uniquely by A, which is fixed.

Next, we prove that $\bar{y} = \bar{x} + \delta x + o(|\delta x|)$. Let $\delta X = \mathrm{diag}(\delta x)$, and observe that

$$\begin{aligned}
&\Big[I - (I - \bar{X} - \delta X)(B' + \delta B)\Big](\bar{x} + \delta x) \\
&\quad = \Big[I - (I - \bar{X})B'\Big]\bar{x} + \delta X B'\bar{x} - (I - \bar{X})(\delta B)\bar{x} \\
&\qquad + \Big[I - (I - \bar{X})B'\Big]\delta x + \psi(o(|\delta x|)),
\end{aligned} \tag{A.6}$$

where $\psi(o(|\delta x|)) = \delta X B'\delta x + \delta X\delta B(\delta x + \bar{x}) - (I - \bar{X})\delta B\delta x$ contains all of the terms that are of order $|\delta x|^2$. The first term on the right is zero due to Eq. (5). Notice that $B'\bar{x} = (I - \bar{X})^{-1}\bar{x}$ according to Eq. (5), and this is substituted into the second term, where we also use the fact that $\delta X(I - \bar{X})^{-1}\bar{x} = (I - \bar{X})^{-1}\bar{X}\delta x$. Finally, we use the constraint equation Eq. (8) to handle the third term. Hence, we obtain

$$\begin{aligned}
&\Big[I - (I - \bar{X} - \delta X)\Big](B' + \delta B)(\bar{x} + \delta x) \\
&\quad = \delta X(I - \bar{X})^{-1}\bar{x} - (I - \bar{X})\Big[(I - \bar{X})^{-2} - B'\Big]\delta x \\
&\qquad + \Big[I - (I - \bar{X})B'\Big]\delta x + o(|\delta x|) \\
&\quad = \bar{X}(I - \bar{X})^{-1}\delta x - (I - \bar{X})^{-1}\delta x + \delta x + o(|\delta x|) \\
&\quad = o(|\delta x|).
\end{aligned} \tag{A.7}$$

To complete Step 2, recall that the single virus system determines the location of $\bar{y}$. At the endemic equilibrium of Eq. (3b), there holds

$$\bar{y} = (I - \bar{Y})B\bar{y}.$$

Rearranging Eq. (A.7) yields

$$\bar{x} + \delta x + o(|\delta x|) = (I - \bar{X} - \delta X)(B' + \delta B)(\bar{x} + \delta x).$$

In other words, our specific form of B (namely our choice of δB) ensures that, for the equilibrium $(\mathbf{0}_n, \bar{y})$, we have that $\bar{y}$ is equal to $\bar{x}+\delta x$, plus some small perturbation of order $o(|\delta x|)$.

Step 3. We must establish that both survival-of-the-fittest eqilibria are locally exponentially stable, i.e. that $\rho[(I - \bar{X})B] < 1$ and $\rho[(I - \bar{Y})A] < 1$.

Consider the effect of a small perturbation δx in the entries of $\bar{x}$ on the Perron–Frobenius eigenvalue of the nonnegative irreducible matrix $(I - \bar{X})A$; we know the Perron–Frobenius eigenvalue is equal to 1. By Lemma 3 we have (to first order in δ)

$$\rho[(I - \bar{X} - \delta X)A] = \rho[(I - \bar{X})A] - u^\top\delta X A\bar{x} \tag{A.8}$$

Now use the fact that $[(I - \bar{X})^{-1} - A]\bar{x} = \mathbf{0}_n$ to write $\rho[(I - \bar{X} - \delta X)A] = 1 - u^\top\delta X(I - \bar{X})^{-1}\bar{x}$. From Eq. (6), we have that $\rho[(I - \bar{X} - \delta X)A] < 1$ as required.

The other survival-of-the-fittest equilibrium can be handled similarly. Using arguments like those above, it is evident that $\rho[(I - \bar{X})(B' + \delta B)] < 1$ if and only if

$$v^\top(I - \bar{X})(\delta B)\bar{x} < 0 \tag{A.9}$$

Using the expression for $(\delta B)\bar{x}$ from Eq. (8), we have that an equivalent condition to Eq. (A.9) is $v^\top[(I - \bar{X})^{-1} - (I - \bar{X})B']\delta x < 0$. Recall that $v^\top$ is the positive left eigenvector of $I - (I - \bar{X})B'$ corresponding to the zero eigenvalue, and so the equivalent condition is

$$v^\top[(I - \bar{X})^{-1} - I]\delta x = v^\top(I - \bar{X})^{-1}\bar{X}\delta x < 0 \tag{A.10}$$

This is guaranteed by Eq. (7). □

Proof of Lemma 2. We postpone the proof that $\rho(B') > 1$ to the end of the following argument.

Observe first that because $\bar{x} > \mathbf{0}_n$, it follows that z must have both positive and negative entries to satisfy $z^\top\bar{x} = 0$. Next, note that

$$[I - (I - \bar{X})B']\bar{x} = [I - (I - \bar{X})(A + \epsilon e_i z^\top)]\bar{x} = \mathbf{0}_n. \tag{A.11}$$

The irreducibility of A implies that there exists a $k \in \mathcal{V}$ such that $a_{ik} > 0$. It follows that for sufficiently small $\epsilon > 0$, $B' = A + \epsilon e_i z^\top$ is nonnegative and irreducible since for any $j \in \mathcal{V}$, $z_j < 0$ only if $a_{ij} > 0$. Therefore B' fulfills Eq. (5). We let $u^\top$ and $v^\top$ be positive left eigenvectors of $-I+(I-\bar{X})A$ and $-I+(I-\bar{X})B'$, respectively, associated with the simple zero eigenvalue (see Lemma 1). Notice that this also implies that $u^\top$ and $v^\top$ are positive left eigenvectors of the nonnegative irreducible matrices $(I - \bar{X})A$ and $(I - \bar{X})B'$, respectively, associated with the Perron–Frobenius eigenvalue, which is equal to unity. We now need to prove that u and v are linearly independent.

Now, assume, to obtain a contradiction, that u and v are in fact linearly dependent. Then $u^\top$ must be a left eigenvector of $(I - \bar{X})B'$ with eigenvalue 1. Observe however that this would imply

$$\begin{aligned}
u^\top = u^\top(I - \bar{X})B' &= u^\top(I - \bar{X})(A + \epsilon e_i z^\top) \\
&= u^\top + u^\top(I - \bar{X})\epsilon e_i z^\top
\end{aligned}$$

Since $u^\top$ and $\mathbf{1}_n$ are positive vectors, $(I - \bar{X})$ is a positive diagonal matrix, and $z^\top \neq \mathbf{0}_n$, it follows that $u^\top(I - \bar{X})\epsilon e_i z^\top = u_i(1 - \bar{x}_i)\epsilon z^\top \neq \mathbf{0}_n$. A contradiction is immediate. Lastly, the fact that $\bar{X}$ is positive definite with diagonal entries less than 1 ensures that $\rho(B') > \rho((I - \bar{X})B') = 1$ (see Item 4 of the properties of M-matrices and Metzler matrices in Section 3). □

References

[1] H.W. Hethcote, SIAM Rev. 42 (4) (2000) 599–653.
[2] R.M. Anderson, R.M. May, Infectious Diseases of Humans, Oxford University Press, 1991.
[3] W. Wang, Q.-H. Liu, J. Liang, Y. Hu, T. Zhou, Phys. Rep. 820 (2019) 1–51.
[4] S. Gracy, M. Ye, B.D.O. Anderson, C.A. Uribe, 2023 American Control Conference, ACC, IEEE, 2023, pp. 2313–2318.
[5] M.E. Newman, C.R. Ferrario, PLoS One 8 (8) (2013) e71321.
[6] W. Cai, L. Chen, F. Ghanbarnejad, P. Grassberger, Nat. Phys. 11 (11) (2015) 936–940.
[7] S. Gracy, P.E. Paré, J. Liu, H. Sandberg, C.L. Beck, K.H. Johansson, T. Başar, Note: Accepted in Automatica (2024) https://arxiv.org/pdf/2207.11414.pdf.
[8] C. Castillo-Chavez, W. Huang, J. Li, SIAM J. Appl. Math. 59 (5) (1999) 1790–1811.
[9] F.D. Sahneh, C. Scoglio, Phys. Rev. E 89 (6) (2014) 062817.
[10] A. Santos, J.M. Moura, J.M. Xavier, IEEE Trans. Netw. Sci. Eng. 2 (1) (2015) 17–29.
[11] J. Liu, P.E. Paré, A. Nedich, C.Y. Tang, C.L. Beck, T. Başar, IEEE Trans. Autom. Control 64 (12) (2019) 4891–4906.
[12] M. Ye, B.D.O. Anderson, J. Liu, SIAM J. Control Optim. 60 (2) (2022) S323–S346, Special Section: Mathematical Modeling, Analysis, and Control of Epidemics.
[13] C. Castillo-Chavez, H.W. Hethcote, V. Andreasen, S.A. Levin, W.M. Liu, J. Math. Biol. 27 (3) (1989) 233–258.
[14] X. Wei, N.C. Valler, B.A. Prakash, I. Neamtiu, M. Faloutsos, C. Faloutsos, IEEE J. Sel. Areas Commun. 31 (6) (2013) 1049–1060.
[15] N.J. Watkins, C. Nowzari, V.M. Preciado, G.J. Pappas, IEEE Trans. Control Netw. Syst. 5 (1) (2016) 298–307.

[16] L.-X. Yang, X. Yang, Y.Y. Tang, IEEE Trans. Netw. Sci. Eng. 5 (1) (2017) 2–13.
[17] R. van de Bovenkamp, F. Kuipers, P. Van Mieghem, Phys. Rev. E 89 (4) (2014) 042818.
[18] A. Santos, J.M. Moura, J.M. Xavier, 2015 49th Asilomar Conference on Signals, Systems and Computers, IEEE, 2015, pp. 1323–1327.
[19] P.E. Paré, J. Liu, C.L. Beck, A. Nedić, T. Başar, Automatica 123 (2021) 109330.
[20] A. Janson, S. Gracy, P.E. Paré, H. Sandberg, K.H. Johansson, Networked multi-virus spread with a shared resource: Analysis and mitigation strategies, 2020, arXiv preprint arXiv:2011.07569.
[21] Y. Wang, G. Xiao, J. Liu, New J. Phys. 14 (1) (2012) 013015.
[22] M. Ye, B.D.O. Anderson, IEEE Control Syst. Lett. 7 (2022) 545–552.
[23] A.S. Ackleh, L.J. Allen, Discrete Contin. Dyn. Syst. Ser. B 5 (2) (2005) 175.
[24] B.D.O. Anderson, M. Ye, SIAM J. Appl. Dyn. Syst. 22 (4) (2023) 2856–2889.
[25] A. Berman, R.J. Plemmons, Nonnegative Matrices in the Mathematical Sciences, in: Computer Science and Applied Mathematics, London, Academic Press, 1979.
[26] A. Santos, Bi-virus Epidemics over Large-scale Networks: Emergent Dynamics and Qualitative Analysis (Ph.D. thesis), Carnegie Mellon University, 2014.
[27] P.E. Paré, J. Liu, C.L. Beck, B.E. Kirwan, T. Başar, IEEE Trans. Control Syst. Technol. 28 (1) (2020) 79–93.
[28] A. Fall, A. Iggidr, G. Sallet, J.-J. Tewa, Math. Model. Nat. Phenom. 2 (1) (2007) 62–83.
[29] A. Lajmanovich, J.A. Yorke, Math. Biosci. 28 (3) (1976) 221–236.
[30] V. Doshi, S. Mallick, et al., IEEE/ACM Trans. Netw. (2022).
[31] W. Mei, S. Mohagheghi, S. Zampieri, F. Bullo, Annu. Rev. Control 44 (2017) 116–128.
[32] P.V. Mieghem, J. Omic, R. Kooij, IEEE/ACM Trans. Netw. 17 (1) (2009) 1–14.
[33] R.A. Horn, C.R. Johnson, Topics in Matrix Analysis, Cambridge University Press, 1994.
[34] Z. Qu, Cooperative Control of Dynamical Systems: Applications to Autonomous Vehicles, Springer Science & Business Media, 2009.
[35] M. Ye, J. Liu, B.D.O. Anderson, M. Cao, IEEE Trans. Autom. Control 67 (4) (2022) 1609–1624.
[36] H.-D. Chiang, L.F.C. Alberto, Stability Regions of Nonlinear Dynamical Systems: Theory, Estimation, and Applications, Cambridge University Press, 2015.
[37] F. Parino, L. Zino, M. Porfiri, A. Rizzo, J. R. Soc. Interface 18 (175) (2021) 20200875.
[38] L. Hogben, Handbook of Linear Algebra, CRC Press, 2006.